Structural characterization of epitaxial α-derived FeSi$_2$ on Si(111)

N. Jedrecy

Laboratoire d'Utilisation du Rayonnement Electromagnétique, Batiment 209D,
Centre Universitaire Paris–Sud, 91405 Orsay Cedex, France
and Laboratoire de Minéralogie-Cristallographie, Universités Paris VI et VII, 4 place Jussieu, 75252 Paris-Cedex 05, France

A. Waldhauer

Laboratoire d'Utilisation du Rayonnement Electromagnétique, Batiment 209D,
Centre Universitaire Paris–Sud, 91405 Orsay Cedex, France
and Département de Recherche sur l'Etat Condensé, les Atomes et les Molécules/Service de Recherche
sur les Surfaces et l'Irradiation de la Matière, Centre d'Études Nucléaires de Saclay, F-91190 Gif-sur-Yvette, France

M. Sauvage-Simkin

Laboratoire d'Utilisation du Rayonnement Electromagnétique, Batiment 209D,
Centre Universitaire Paris–Sud, 91405 Orsay Cedex, France
and Laboratoire de Minéralogie-Cristallographie, Universités Paris VI et VII, 4 place Jussieu, 75252 Paris-Cedex 05, France

R. Pinchaux

Laboratoire d'Utilisation du Rayonnement Electromagnétique, Batiment 209D,
Centre Universitaire Paris–Sud, 91405 Orsay Cedex, France
and Université Pierre et Marie Curie, 4 place Jussieu, F-75252 Paris-Cedex 05, France

Y. Zheng

Laboratoire de Minéralogie-Cristallographie, Universités Paris VI et VII, 4 place Jussieu, 75252 Paris-Cedex 05, France
(Received 1 September 1993)

The tetragonal symmetry of epitaxial FeSi$_2$ grains on Si(111) has been revealed for thin films (< 40 Å) issued from two very different processes, which had in common a growth temperature of about 500 °C. The structure has been investigated by out-of-plane x-ray diffraction and transmission electron microscopy. An atomic model is proposed derived from the high-temperature α phase.

I. INTRODUCTION

Among transition-metal silicides, the Fe-Si system appears of particular interest for two reasons. First, the β-FeSi$_2$ silicide stable at low temperature with a direct gap of 0.87 eV could be used as a constituent in Si-based optoelectronic devices,[1] provided that the quality of epitaxial films can be improved. Second, some new iron silicide phases stabilized by the strain induced by epitaxy on Si(111) substrates have recently been identified.[2-4] These metastable phases could perhaps be used as precursors to achieve Si-β heterostructures. They would exist in the stoichiometric range FeSi$_{1+x}$, $0 < x < 1$. Their existence is dependent on the growth procedure, the substrate temperature, and the overlayer thickness. However, their epitaxy, as well as that of the corresponding bulk compounds, seems to proceed in a common fashion: the stacking along the Si surface normal direction of atomic layers with a quasihexagonal two-dimensional (2D) cell, this stacking being rotated by 180° about the normal from the Si one. This would indicate that growth is controlled by specific atomic interactions at the interface.

The Si(111) crystal may be described as double layers stacked along the surface normal in a face-centered-cubic (fcc) way (the so-called *ABC* stacking). The 2D lattice cell is simply hexagonal and is referred to as 1×1. Due to the 6 mm symmetry of each Si (111) layer coupled to the $3m$ symmetry of the bulk projection, a cubic compound with a lattice constant equal or close to a fraction of the silicon one may develop two types of (111) epitaxy. The (111) 2D lattice cell of the epilayer will fit with the Si one, while the stacking along the normal will be on line or rotated by 180° about the [111] axis with respect to the silicon substrate. These two different azimuthal orientations are referred to as "type A" and "type B," respectively. For an epilayer with no ternary axis normal to the interface, three equivalent domains rotated by ±120° from one another are expected in each case. We have characterized by x-ray diffraction (XRD) and high-resolution transmission electron-microscopy (HRTEM) a new metastable phase derived from the high-temperature ($T > 940$ °C) α-FeSi$_2$ bulk form.[5] This phase was identified on two very different samples. A solid phase epitaxy (SPE) process on a 10 Å iron deposit, heated up to 500 °C, has resulted mainly in α-derived islands of 30 Å height, with a type B orientation. Similar results were obtained with a sample grown by metal-organic chemical-vapor deposition (MOCVD). The α-type

tetragonal symmetry has also been reported, by Chevrier et al.,[4] on the basis of reflection high-energy electron diffraction (RHEED) and in-plane XRD data, for films issued from 10 Å deposits at 550 °C, and by Lin et al.,[6] for precipitates formed by the ion beam-induced epitaxial crystallization (IBIEC) process. A quantitative analysis of our x-ray data allows us to propose a unit-cell model derived from the high-temperature α phase. In addition, we detected a 2D thin epilayer in the SPE sample, which, on account of HRTEM images alone, is compatible with both the α structure and the $FeSi_{1+x}$ cubic one proposed by von Känel et al.[3]

A preliminary description of the main epitaxial phases on Si(111) will be given, which establishes the connection between the different stoichiometries. The orientation relationship of the α-derived phase will then be discussed, and complemented by a structure proposal based on Bragg intensity values.

II. THE DIFFERENT EPITAXIAL SILICIDES UNDER CONSIDERATION

The most Fe-rich bulk silicide is Fe_3Si, which crystallizes with a cubic structure (mismatch of $+3.93\%$ with Si). It consists in a fcc iron sublattice with all octahedral sites occupied by Fe atoms and all tetrahedral sites occupied in equal proportion by both Fe and Si atoms. The structure resulting from a random occupation of the tetrahedral sites is simple cubic with a lattice constant close to half the silicon one (5.431 Å), while the ordered occupation leads to the same fcc lattice as in silicon. The Fe_3Si stoichiometry was evidenced in room-temperature interfaces with Si(100) substrates.[6] To our knowledge, it has not been reported on Si(111), but the (111) epitaxy with an alignment of $\langle 011 \rangle$ in-plane axes should be the logical accommodation. The following bulk compound is FeSi (referred to as ε-FeSi), which adopts a complicated cubic structure.[7] The lattice misfit with Si is $+17.36\%$ but the (111) epitaxy may be found with azimuthal orientation $\langle 11\bar{2} \rangle^{\varepsilon\text{-FeSi}}\|\langle 01\bar{1} \rangle^{Si}(-4.58\%)$. The resulting in-plane cell is $\sqrt{3}\times\sqrt{3}$-R 30°-like, but a close inspection of the atomic configuration shows that the (111) layers have a distorted 2D Si-type 1×1 cell, except every fourth layer, which can be considered as a "rough" mixed layer, with both occupation factors for Si and Fe on the 1×1 sites equal to $\frac{1}{2}$. The 2D cell associated to these partially filled layers is 3×3. The layers are stacked in a particular ABC fashion, the Fe interlayer distance being slightly smaller than $a^{Si}\sqrt{3}/6$. Evidence of a unique type of epitaxial orientation, related to a B-type interface, is given in Ref. 8. The next bulk silicide is β-$FeSi_2$ which displays an orthorhombic symmetry. An extended structural study of its epitaxy on Si(111) is given in Ref. 8. The silicide interfacial planes are mostly (101) and (110) planes, which can be related to the (111) planes of a CaF_2-type (fluorite) structure, in a type B orientation. The Fe(111)-type layers are at a distance of about $a^{Si}\sqrt{3}/3$. The corresponding fluorite cell is a fcc Fe unit with all tetrahedral sites occupied by Si, and a parameter value comparable to that in silicon. As a matter of fact, this

fluorite structure is one of the metastable phases (referred to as γ-$FeSi_2$), but it was observed only on limited regions in a narrow thickness and temperature range.[9] The $FeSi_2$ stoichiometry was also observed with a simple cubic structure, the lattice parameter being half the silicon one.[3] This last structure would exist with a stoichiometry ranging from FeSi to $FeSi_2$ and can be derived from the CsCl-type structure (that is a Si cubic cell whose center is occupied by an Fe atom). Starting from FeSi, the stoichiometry evolves towards $FeSi_2$ by introducing vacancies in a random fashion in the Fe sublattice. In this case also, the type B (111) orientation alone is reported.[3] The Fe interlayer distance is $a^{Si}\sqrt{3}/6$ for all stoichiometries as (approximately) in the ε bulk case. The α-$FeSi_2$ phase crystallizes above 940 °C with a tetragonal structure ($a = 2.684$ Å and $c = 5.128$ Å).[5] We may consider for the sake of clarity a cubic unit cell with an average parameter value of 5.311 Å (misfit of -2.21% with Si). The structure is obtained from the fluorite one, first by filling all the octahedral sites with Fe, then by removing energy second (001) Fe plane. In the present work, the (111) type B epitaxy of such a phase (if one considers the cubic cell) was unambiguously characterized although the growth temperature did not exceed 550 °C. The atomic configurations for the CsCl-, CaF_2-, and α-type (111) epitaxies are presented in Fig. 1, in a $(\bar{1}10)$ projection. The CsCl-derived $FeSi_2$ phase is obtained from CsCl-FeSi considering an occupation factor of $\frac{1}{2}$ for Fe sites. The Fe(111) interlayer distance in the α case is the same as in the CsCl-$FeSi_2$ epitaxy, but instead of layers with half sites vacant in a random fashion, an in-plane distribution now takes place leading to (001) slabs alternatively filled. The epitaxial strain is thus expected to be released mainly along the Si in-plane $\langle 112 \rangle$ axis. We note that in the α and ε bulk cases, the close Fe interlayer distance is made possible by some (111) 1×1 vacant sites. No assumption is made for the interface region, but the occurrence of type B orientation in all epitaxies promotes a unique type of bonding. Despite the similarities in the (111) stacking of layers through a common cubic Si environment around the Fe atoms, Fig. 1 makes clear that important atomic displacements are necessary to induce transitions from one phase to another. As a matter of
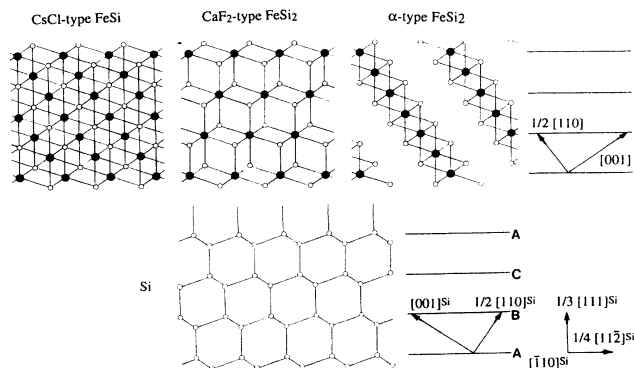
FIG. 1. Projection along $[\bar{1}10]^{Si}$ of the CsCl-, CaF_2-, and α-type (111) epitaxial silicides on Si(111) with a B-type orientation.

fact, the transition from $CsCl$-$FeSi_2$ to β-$FeSi_2$ (close to CaF_2 type) obtained by annealing (550 °C) was found to proceed via an intermediate decrease of the crystalline order in the bulk.[10] On the contrary, the transition from $CsCl$-$FeSi_2$ to ϵ-$FeSi$ with a deposition of iron at about 350 °C has been reported to arise with coexisting well-ordered phases.[11]

The metastable epilayers can easily be detected and identified by out-of-plane diffraction. For the sake of clarity, let us consider all the possibilities using a common cubic unit cell with a parameter value equal to that of Si. Since all observations on the various iron silicides have shown a type B epitaxy, the orientation relationship of the epilayer is supposed to be $(111)^e\|Si(111)$ with $[1\bar{1}0]^e$ along $[\bar{1}10]^{Si}$. This characterizes a single domain, with the other two, when the symmetry is lower than in silicon, being obtained through rotations of $\pm120°$. The reciprocal lattice (RL) nodes of such a cubic or pseudocubic type B epilayer together with the Si nodes are presented in Fig. 2, for $(\bar{1}10)^*$ and $(11\bar{2})^*$ cross sections. In the case of a fcc lattice for the epilayer, only hkl reflections with h,k,l of the same parity are allowed (those at 180° about the normal from the Si ones in Fig. 2). This is valid for the fluorite $FeSi_2$. It should be noted that, in the case of a type A orientation for which $FeSi_2$ and Si reflections would be superposed, x-ray measurements of particular reflections forbidden in silicon, such as 002, could reveal

the presence of the epilayer.

In $FeSi_{1+x}$, since the true lattice parameter is $a = a^{Si}/2$, all hkl reflections with one odd index are forbidden. For α-$FeSi_2$, the true unit cell is tetragonal with $a = b = a^{Si}/2$ and $c = a^{Si}$, then all hkl reflections with h or k odd are forbidden. Compared with the $FeSi_{1+x}$ case, reflections with 1 odd are now allowed. The $FeSi_{1+x}$ and α-$FeSi_2$ reflections are displayed in Fig. 2.

III. SAMPLE PREPARATION

The SPE process was carried out under ultrahigh vacuum conditions using an electron beam iron evaporator. We started with a 5 Å equivalent Fe deposit at room temperature on a Si(111) 7×7 surface. The sample was annealed up to 500–550 °C through radiative heating from a tungsten filament. The procedure lasted 10 min, the time needed due to inertia to reach 500 °C. These conditions were chosen so as to get the 2×2 reconstruction, which is associated to a strained cubic phase. Sirringhaus et al.,[10] as well as Motta et al.,[12] concluded from scanning tunneling microscopy (STM) analysis that this reconstruction would terminate $CsCl$-type domains, on the basis of surface step height equal to 1.6 Å ($a^{Si}\sqrt{3}/6$). Our initial purpose was to obtain quantitative information on this phase and the 2×2 structure. In layers of that thickness, we observed that a progressive heating process always leads to both 2×2 and $\sqrt{3}\times\sqrt{3}$-R 30° (ϵ-$FeSi$) RHEED features. This last structure cannot be eliminated unless long-time annealing about 550 °C or high-temperature heating are performed, which produce the β-$FeSi_2$ formation. The results of a grazing incidence XRD experiment on the 2×2 reconstruction will be discussed in a forthcoming publication.[13]

The first 5 Å deposit was followed by a second one (5 Å) with a lower-temperature annealing (450 °C). This resulted in a blurred 2×2 RHEED pattern with additional streaks indicating facets formation. We expected a final 30 Å film; however, the TEM analysis revealed that the average thickness was somewhat smaller. The sample was protected with an amorphous GaAs layer.

The second sample was the result of a codeposition process at 540 °C under H_2 atmosphere, using $Fe(CO)_5$ and Si_2H_6 compounds. The thickness of the rather homogeneous film was around 40 Å.

IV. X-RAY EVIDENCE OF THE α TETRAGONAL SYMMETRY OF THE SILICIDE

We performed θ-2θ scans (radial scans) across each significant position in the reciprocal space, using a full four-circle diffractometer. The experiment was carried out at the D25 beam line of the LURE synchrotron radiation facility (Orsay, France). We used a Si(111) channel-cut monochromator to select, first, the wavelength at Ni K edge ($\lambda = 1.488$ Å). The third harmonic ($\lambda/3$) is also generated, and can be separately analyzed by the use of an energy-sensitive detector. On the two samples, the peaks measured at 001 and 021 positions (see Fig. 2) prove the existence of the α phase, or at least of a similar tetragonal lattice for the epilayer. For each
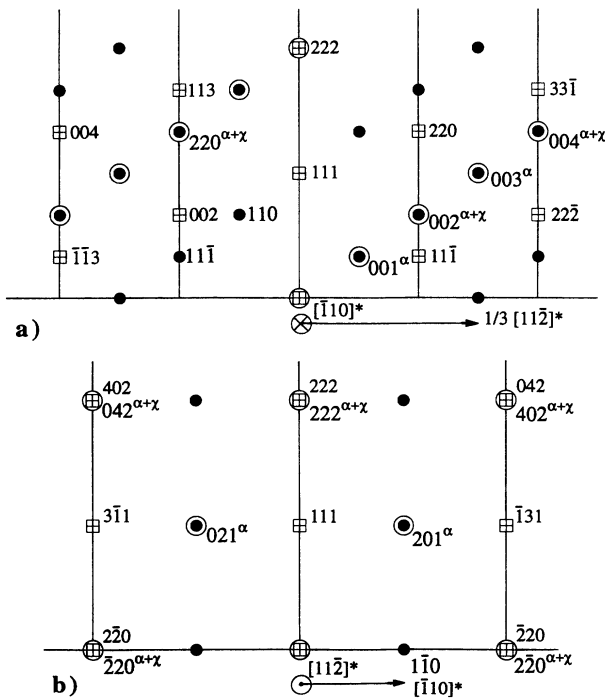
FIG. 2. Cross sections of the reciprocal space, containing the origin, and assuming a cubic B-type (111) epitaxial silicide on Si(111), with the same lattice constant: (a) perpendicular to $[\bar{1}10]^{Si}$; (b) perpendicular to $[11\bar{2}]^{Si}$. The squares refer to Si, the black dots to a simple cubic silicide. The large circles denote reflections expected in the α tetragonal case. Those common with the $FeSi_{1+x}$ phase are denoted by the index χ.

reflection, an equivalent was found at $\pm 120°$, as expected from the Si $3m$ symmetry. The 110 and $11\bar{1}$ positions did not reveal any peak, thus eliminating the possible existence of a simple cubic phase or of an fcc compound with $a = a^{Si}$. The $FeSi_{1+x}$ phase has common reflections with the α-derived phase, but, as will be presented in the next section, it does not contribute in a measurable way to the collected Bragg intensities. However, this phase could occur for thin 2D regions with apparent distortions detected by use of HRTEM (see Sec. V).

With out-of-plane scans, an accurate determination of the location of Bragg nodes is quite difficult. Nevertheless, with the SPE sample, we could detect the respective third harmonics of $88\bar{4}^{Si}$ when scanning across the 004^{α} reflection and of 228^{Si} when scanning across the 220^{α} reflection. We first performed θ-2θ scans across the positions at $180°$ from 004^{Si} and 220^{Si}. On such scans, we detect both α and Si peaks at the same angle. On the contrary, performing an excursion along each respective Si rod, we observed that the maxima of intensity for the α peaks were, respectively, at $\overline{0.02, 0.02}$, 3.98 and 2.02, 2.02, 0.02. The ϕ scans (rotation of the sample around the surface normal) across each position confirmed that the α nodes were very close to the Si rods (at $\pm 0.05°$). This leads us to conclude that the (111) α planes are tilted $(0.8°)$ with respect to the Si(111) surface, and that compared to the Si reticular distances, the α(001) distance is larger while the α(110) one is smaller. This is unexpected since the reported α-bulk lattice constants give a nearly cubic cell with all parameter values smaller than in Si: $a^{\alpha} = b^{\alpha} = 5.368$ Å and $c^{\alpha} = 5.128$ Å, compared with $a^{Si} = 5.431$ Å. The a and c lattice constants for the SPE epilayer would be equal, respectively, to 5.377 and 5.458 Å. With the MOCVD sample, the Si harmonics were apparent in one ϕ scan alone, which revealed a $\Delta\phi$ between the 004^{α} and $88\bar{4}^{Si}$ nodes of $0.2°$. The c parameter value was estimated from other scans to be between 5.411 and 5.445 Å, which, as in the SPE case, is larger than expected. These findings support the assumption of additional (001) Fe planes in the metastable α phase, inferred from the analysis of Bragg intensities (see Sec. VI). Indeed, while the weak 002 reflection could be measured with the 40 Å MOCVD film, we could not detect any signal for the 003 reflection in the two samples. This was confirmed on transmission electron diffraction (TED) patterns. Modifications in the α-bulk structure thus had to be considered.

The coherent domain sizes for the SPE and MOCVD epilayers, estimated from the scans, revealed similar, about 100 Å in-plane (θ-2θ scans), and about 30 Å in the surface normal direction (rod scans).

V. THE HRTEM ANALYSIS

Intriguing HRTEM features are observed with the tetragonal epitaxial phase. The analysis was performed by use of a TOPCON EM 002B microscope (200 kV) on cross sections prepared by mechanical thinning and an Ar^+ ion-beam technique. Two cross sections of the SPE sample with the electron beam along $[\bar{1}10]^{Si}$ and $[11\bar{2}]^{Si}$ are presented in Figs. 3 and 4, respectively. The
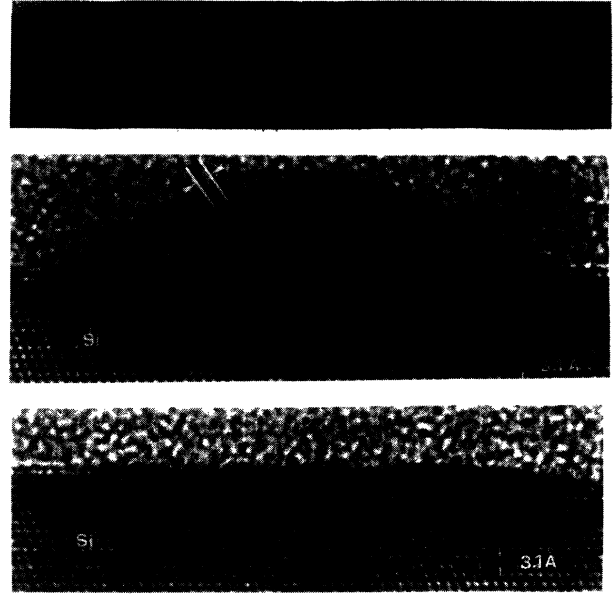
FIG. 3. TEM cross section with the electron beam along $[\bar{1}10]^{Si}$. Magnified views of the island and the 2D thin epilayer are presented below. For the island, the α(001) and (220) interplanar distances are outlined by white and black streaks, respectively.

MOCVD sample gave the same kind of images, except that the film consisted of adjacent grains about 40 Å high and 100 Å wide, covering the whole surface. The island in Fig. 3 has dimensions close to those of the MOCVD grains. It clearly displays (001) and (220) α planes, as expected from the reciprocal lattice given in Fig. 2. A flat apparently distorted silicide layer extends on top of the remaining Si zones, and will be analyzed later on. The micrograph in Fig. 4 reveals only $(2\bar{2}0)$ planes, while, if referring to Fig. 2 and to the microscope resolution of 0.18 nm, (021) and (201) planes should be visualized. This could be explained by the presence of three α domains. Indeed, the RL cross sections in Fig. 2 are issued from the choice of [001] at $180°$ from $[001]^{Si}$. We should have considered due to the $3m$ substrate symmetry the two others possibilities, that is, [010] or [100] at $180°$ from $[001]^{Si}$. In such epitaxial grains, the $(0\bar{2}2)$ or $(20\bar{2})$ planes alone are expected to be reconstituted in the $(11\bar{2})^{Si}$ TEM image (the reflections 102 as 210 are forbidden). However, transmission electron diffraction (TED)

FIG. 4. TEM cross section with the electron beam along $[11\bar{2}]^{Si}$ of an α island. The α(220) planes alone are reconstituted in the image.

patterns could be obtained with the MOCVD sample. The 021 and 201 reflections were clearly excited implying that the reconstituted image should display {021} planes. We never could observe those planes.

Considering the possible orientation [010] (or [100]) at 180° about the normal from $[001]^{Si}$, a $(\bar{1}10)$ TEM cross section should display (020) or (200) planes, with a reticular distance half the one apparent in Fig. 3 (the reflections 010 and 100 are forbidden). We effectively obtained such images. On the MOCVD sample, {001} and {002} planes could even be resolved on a single image depending on the grains. A surprising feature is their occurrence when changing the electron focalization conditions on the island of Fig. 3. The $(\bar{1}10)^*$ TED patterns from the MOCVD sample revealed that the 002 reflection was really more intense than the 001 one, when the inverse is expected from the α bulk structure. They confirmed that the 003 reflection was absent. These two features make possible confusion, in the case of low silicide thickness, between such a tetragonal epilayer and the cubic $FeSi_{1+x}$ phase, if a TEM analysis alone is performed.

Concerning the flat 2D film in the SPE sample (see Fig. 3), we can recognize {002}- and {220}-type planes despite some distortions in the lattice. On account of the above description, no conclusion can be made on the true nature of this epilayer. However, the different morphology and contrast, with respect to the islands, favor the $FeSi_{1+x}$ description with x closer to 0 than to 1. The magnified view in Fig. 3 shows a very abrupt interface with disruption of $Si(11\bar{1})$ planes when the (002) interplanar distance is preserved. This kind of interface is observed in the right half part of the island, as if its growth has started from a similar 2D region and has extended laterally.

VI. THE α-DERIVED MODEL PROPOSAL

The absence of any measurable signal at the 003 position leads us to consider deviations from the α-bulk reported structure. We first calculated the structure factors expected from such a structure, allowing distortions in the Si sublattice alone. The α-bulk unit cell has already been described; starting from the CsCl-type structure with lattice constant $a^{Si}/2$, every second (001) Fe plane has to be removed. The Si atoms were allowed to move along the [001] direction from tetrahedral positions, in a symmetrical way from the (001) Fe planes. This preserves the tetragonal symmetry and the $FeSi_2$ stoichiometry. The Si atom coordinates along the c axis are equal respectively to $\frac{1}{4}+\Delta z$ and $\frac{3}{4}-\Delta z$. We took into account the presence of the three orientations in equal proportion. This leads us to attribute a different weight for reflections with even l index (a single domain contributes to reflections with odd l index). The experimental intensities are compared with the model in Fig. 5, after appropriate corrections. The intensity is calculated as a function of Δz^{Si}. A signal for the 002 reflection could only be detected with the MOCVD sample; the experimental point is superposed with 021 in the figure. The major characteristics of the α phase are reproduced at
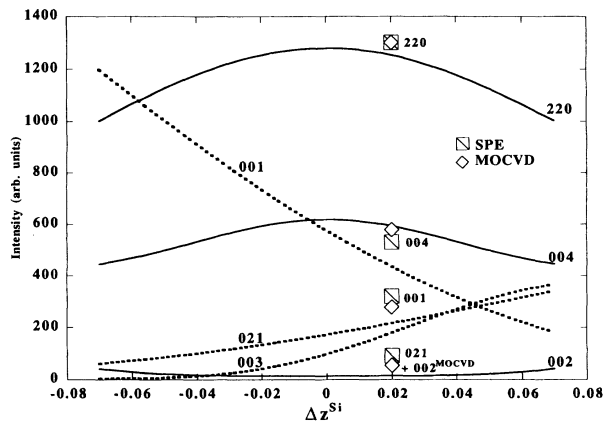
FIG. 5. The evolution of the expected diffracted intensity for several α reflections with Δz^{Si}, where Δz^{Si} is the deviation along [001] of the Si coordinates from the tetrahedral positions. Experimental points are displayed.

about $\Delta z^{Si} = +0.02$, which is the reported bulk value. No error bars are given for the experimental intensities because of difficulty in evaluating them. Indeed, they range from 7% to 20% depending on reflections and the way comparisons are made. Two effects have to be considered. First, the scans are performed with different diffractometer angles (the θ Bragg angle and the χ angle between the momentum transfer and the silicon surface). The diffracted intensity depends on the sample area which is irradiated on account of these two angles. We used slits in front of the incident x-ray beam to limit this effect. Second, the integrated intensities of the 001, 002, and 021 reflections were extracted from scans with a nonlinear background level which precludes in the case of low signals an accurate determination of the intensity. However, the 003 reflection could never be measured, while this model predicts an intensity of the same order of magnitude as for 021, which was unambiguously detected with both samples. We thus tried to modify the structure so as to affect only reflections with odd l index. This can be achieved by a new distribution of the Fe atoms, introducing additional (001) planes at $c/2$. The stoichiometry was preserved considering an occupation factor equal to p for the sites of the intermediate planes, and equal to $1-p$ for the others. The new evolution with Δz^{Si} of the 001, 003, and 021 reflections, for three different p values ($\frac{1}{8}$, $\frac{1}{4}$, and $\frac{3}{8}$, respectively), is presented in Fig. 6. A broad minimum of the 003 intensity is found at $\Delta z^{Si} = -0.03$ in each case. The 001 reflection is the most sensitive and leads us to conclude to a p value of $\frac{1}{4}$, that means occupation factors equal alternatively to $\frac{1}{4}$ and $\frac{3}{4}$ in the successive Fe(001) layers. A good agreement is also found with $\Delta z^{Si} = -0.02$ if a p value of $\frac{1}{6}$ is considered. Coming back to Fig. 5, these two Δz^{Si} values are as convenient as the positive one when considering reflections with even l index. On account of the a and c parameter values determined with the SPE sample, the Fe-Si distance would be of 2.28 Å for the Fe atoms from the (001) planes with $p = \frac{1}{6}$ and of 2.40 Å for the others.
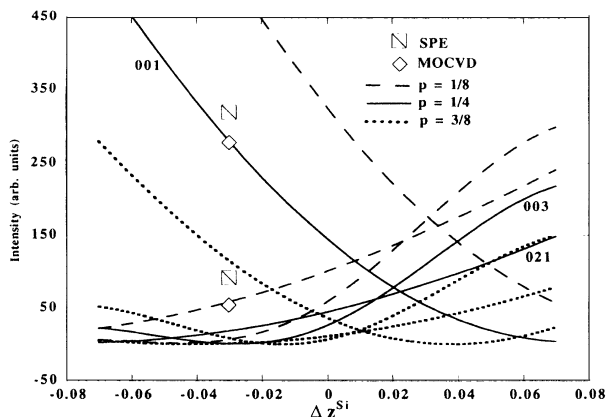
FIG. 6. Same as in Fig. 5, for three different p values of the occupation factors in the half integral (001) Fe planes. Only the intensities of reflections with odd l index are represented. The full lines correspond to $p = \frac{1}{4}$, the dashed lines to $p = \frac{1}{8}$, the dotted lines to $p = \frac{3}{8}$.

This agrees with the Fe-Si distance in the α-bulk phase (2.35 Å).

We also performed several scans at different photon energies around the Fe K edge. As some new parameters have to be included for the calculation of Bragg intensities (the anomalous dispersion corrections to the Fe atomic scattering factor), we cannot use them to conclude between the two models. In any event, the raise in intensity expected for the 002 reflection at the Fe K edge was observed, together with the decrease for the other reflections.

VII. CONCLUSION

The α-derived model we propose for the tetragonal epitaxial phase provides a hint in understanding the transition observed by Chevrier *et al.*[5] from α-FeSi$_2$ to β-FeSi$_2$ with increasing thickness. This last phase is understood as a Jahn-Teller distortion of the CaF$_2$-type structure, which is obtained from the α-bulk one by relocating half of the atoms from the (001) Fe layers into the available interplanar (001) regions (see Fig. 1). This should occur in an ordered fashion so as to suppress every second $\alpha(111)$ Fe layer. We have specified in Ref. 8 the role of the $\beta(100)$ orientation in the growth mechanism. Indeed, (100) [011]/2 stacking faults were shown to occur as frontiers between alternate slabs of epitaxial (101) and (110) β-FeSi$_2$ on Si(111). This $\beta(100)$ orientation is to be related to the (001) one of a cubic-(111) B-type epilayer. Thus, the α-derived phase we have evidenced could be a precursor state for further β growth. The analysis by HRTEM of the evolution of island morphology and Si-FeSi$_2$ interface during the α-β transition should be of great interest to confirm this transformation phenomenon.

ACKNOWLEDGMENTS

[1] J. Derrien, J. Chevrier, V. Le Than, and J. E. Mahan, Appl. Surf. Sci. **56/58**, 382 (1992).

[2] N. Onda, J. Henz, E. Müller, K. A. Mäder, H. von Känel, Appl. Surf. Sci. **56/58**, 421 (1992).

[3] H. von Känel, K. A. Mäder, E. Müller, N. Onda, and H. Sirringhaus, Phys. Rev. B **45**, 13 807 (1992).

[4] J. Chevrier, P. Stocker, Le Thanh Vinh, J. M. Gay, and J. Derrien, Europhys. Lett. **22**, 449 (1993).

[5] B. Aronsson, Acta Chem. Scandinavia **14**, 1414 (1960).

[6] X. W. Lin, M. Behar, J. Desimoni, H. Bernas, Z. Liliental-Weber, and J. Washburn, Appl. Phys. Lett. **63**, 105 (1993).

[7] L. Pauling and A. M. Soldate, Acta Cryst. **1**, 212 (1948).

[8] N. Jedrecy, Y. Zheng, M. Sauvage-Simkin, and R. Pinchaux, Phys. Rev. B **48**, 8801 (1993).

[9] H. von Känel, N. Onda, H. Sirringhaus, E. Müller-Gubler, S. Goncalves-Conto, and C. Schwarz, Appl. Surf. Sci. **70/71**, 559 (1993).

[10] H. Sirringhaus, N. Onda, E. Müller-Gubler, P. Müller, R. Stalder, and H. von Känel, Phys. Rev. B **47**, 10 567 (1993).

[11] Le Thanh Vinh, J. Chevrier, and J. Derrien, Phys. Rev. B **46**, 15 946 (1993).

[12] N. Motta, A. Sgarlata, G. Gaggiotti, F. Patella, A. Balzarotti, and M. De Crescenzi, Surf. Sci. **284**, 257 (1993).

[13] N. Jedrecy, A. Waldhauer, M. Sauvage-Simkin, and R. Pinchaux (unpublished).
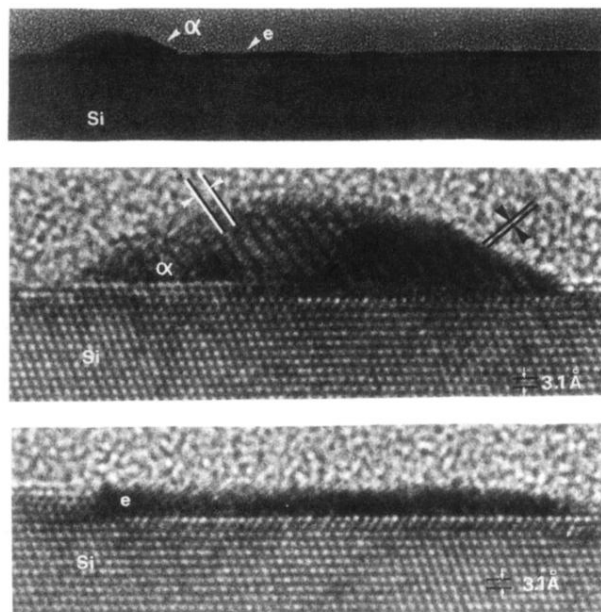
FIG. 3. TEM cross section with the electron beam along $[\bar{1}10]^{Si}$. Magnified views of the island and the 2D thin epilayer are presented below. For the island, the $\alpha(001)$ and (220) interplanar distances are outlined by white and black streaks, respectively.
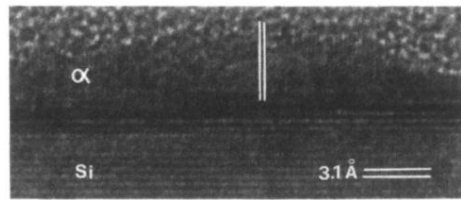
FIG. 4. TEM cross section with the electron beam along $[11\bar{2}]^{Si}$ of an α island. The $\alpha(220)$ planes alone are reconstituted in the image.